Efficient solar cells are more stable: The impact of polymer molecular weight on performance of organic photovoltaics

Z. Ding[a],[†] J. Kettle[a],[†] M. Horie[b], S.W. Chang[b], G.C. Smith[c], A. I. Shames[d], E. A. Katz[e,f]*

The principle remaining challenge in the research area of organic photovoltaic (OPV) materials is to develop solar cells that combine high efficiency, stability and reproducibility. Here, we demonstrate an experimental strategy which has successfully addressed this challenge. We produced a number of samples of the highly efficient PTB7 polymer with various molecular weights (M_n ~ 40 - 220 k). OPV cells fabricated with this polymer demonstrated significant improvement of the cell efficiency (by ~90 % relative) and lifetime (by ~300 % relative) with the M_n increase. We attribute these effects to lower density of recombination centers (radical defects revealed by EPR spectroscopy) and better photoactive layer morphology in the samples with higher M_n. Relevance of the observed correlation between the OPV efficiency and stability is discussed.

1. Introduction

Organic photovoltaics (OPVs) using a bulk heterojunction (BHJ) structure show promise as an alternative to inorganic semiconductors for solar electricity production and have shown power conversion efficiencies (PCE) in excess of 10% [1]. Much of this success has come with conjugated polymer/fullerene combinations via optimization of polymer design and device fabrication procedures [2-4]. Though the operational lifetime of OPVs is much shorter than that of commercial inorganic PV (~25 years for Si devices), significant progress has been made in improving the stability of OPVs [5]. However, the greatest challenge in this research area is to develop OPV devices *combining* high efficiency and stability. Indeed, the record outdoor operational lifetime of ~ 2 years was demonstrated for low-efficient devices (P3HT-PCBM BHJ devices with PCE ~ 1%) [6]. On the other hand, poly({4,8-bis[(2-ethylhexyl)oxy]benzo[1,2-b:4,5-*b'*]dithiophene-2,6-diyl}{3-fluoro-2-[(2-ethylhexyl)carbonyl]thieno[3,4-*b*]thiophenediyl}) (PTB7), an attractive low bandgap polymer [7], is found to exhibit PCE over 7% when blended with the fullerene derivative [6,6]-phenyl C_{71}-butyric acid methyl ester (C_{71}-PCBM) [8] but suffers from poor stability [9, 10, 11].

Another vital drawback of polymer OPVs is poor reproducibility of the physical and electronic properties of polymer-based semiconductors. Different samples of the same polymer might differ by the molecular weight, amount of defects and residual impurities, and consequentially, different polymer batches might perform quite differently in OPV devices [12]. To resolve this limitation an extensive experimental program with a wide international cooperation is currently planned [13].

Recently, Troshin et al suggested that Electron Paramagnetic Resonance (EPR) spectroscopy is a very powerful tool for assessment of the quality of different conjugated polymers used as the electron donor in OPV [12] and monitoring their photochemical and thermal degradation [11]. It has been shown that different batches of the same conjugated polymer might contain substantially different amounts of radical species behaving as traps for mobile charge carriers. Indeed, a correlation between the concentrations of radicals in various batches of conjugated polymers and PCE of the OPV cells on their basis has been revealed [12]. Furthermore, the relative stability of materials was suggested to be quantified from the rates of radical accumulation estimated from their EPR spectra [11].

In this paper, we present photovoltaic performance and lifetime of OPV devices fabricated with PTB7 synthesized by various methods or using different commercial sources. We report that the increase in polymer molecular weight results in decrease of the density of radical defects in the material and corresponding improvement of efficiency and stability of PTB7-based solar cells. We suggest that this relationship may also apply to other conjugated polymers. Furthermore, the study of various grades of the same polymer allows us to postulate a general rule: namely, a more efficient cell should be more stable. Indeed, photoinduced degradation of PV devices under operation is caused by sunlight. The larger the proportion of the incident sunlight power that is converted to electrical power, the smaller the part remaining for activation of degradation. This positive conclusion may be very important for future development of next generation PV.

2. Experimental

2.1 Synthesis of PTB7

2,6-Bis(trimethyltin)-4,8-bis(2-ethylhexyl)benzo[1,2-*b*:3,4-*b'*]dithiophene (66.6 mg, 0.085 mmol) and 2-ethylhexyl-4,6-dibromo-3-fluorothieno[3,2-*c*]thiophene-2-carboxlate (40.0 mg, 0.085 mmol) were dissolved in 0.96 mL *p*-xylene and 0.24 mL dimethylformamide (DMF) in a 5 mL Schlenk tube. Tris(dibenzylidenacetone)palladium(0) (2.3 mg, 0.003 mmol, 5 mol%) was added, and the reaction was stirred at 120 °C for 5.5 hours. Then 0.2 mL 4-bromoanisole was added and stirred at 120 °C for an hour. The resulting mixture was precipitated into a mixture of methanol (100 mL)/37% HCl aqueous solution (2 mL). The precipitate was washed by Soxhlet extraction with ethanol for one day followed by a further day with methylethylketone (MEK), and then extracted with $CHCl_3$. The solution was filtered through a silica gel column (c.a. 1 cm of silica gel in height). The chloroform solutions of the polymer were re-precipitated into methanol and then collected using

centrifugation at 6000 rpm for 1 minute. The precipitates were dried in vacuum to yield deep blue powder **PTB7-1** (57 mg, 89% yield). GPC: M_n = 41200, M_w/M_n = 2.55.

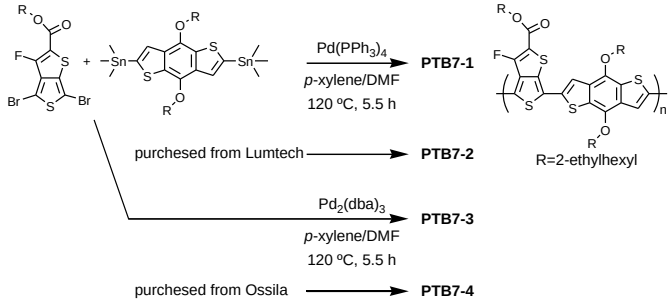

***Scheme 1**. Preparation of PTB7, in order from low (**PTB7-1**) to high molecular weight (**PTB7-4**).*

Similar procedure was applied using tetrakis-(triphenylphosphine)palladium(0) (2.0 mg, 0.003 mmol, 5 mol%) to yield deep blue powder **PTB7-3** (63 mg, 98% yield). GPC: M_n = 108900, M_w/M_n = 2.56. **PTB7-1** obtained from $Pd_2(dba)_2$ catalyst showed lower molecular weight of M_n = 41k than that of PTB7-3 obtained from $Pd(PPh_3)_4$ catalyst (M_n = 109k). The commercial polymers **PTB7-2** and **PTB7-4** showed relatively high molecular weight of M_n = 83k and very high molecular weight of M_n = 216k, respectively.

***Table 1.** Molecular weight, optical[a] and electrochemical[b] properties of polymers*

Polymer	M_n (PDI)	λ_{max} [nm]		E_g	HOMO	LUMO
		Solution	film	[eV][c]	[eV][d]	[eV][e]
PTB7-1	41,200 (2.55)	666	668	1.67	-5.08	-2.95
PTB7-2	83,300 (2.83)	671	670	1.66	-5.12	-3.01
PTB7-3	109,900 (2.56)	647	640	1.57	-5.18	-3.11
PTB7-4	215,700 (2.46)	671	675	1.63	-5.19	-3.10

[a] Measured by UV-vis light spectroscopy. [b] Measured by cyclic voltammetry (CV). [c]Optical band gap. [d] Highest Occupied Molecular Orbital, HOMO = – (4.8 + $E_{pa\text{-}onset}$–E_{Fc}). Half wave potential of ferrocene, E_{Fc} (= 0.845 V vs AgCl/Ag), was measured in MeCN solution. [e] Lowest Occupied Molecular Orbital, LUMO = – (4.8 + $E_{pc\text{-}onset}$–E_{Fc}).

2.2 Material characterisation

Molecular weight and polydispersity index (PDI) of the polymers were measured by gel permeation chromatography (GPC) using THF as an eluent and polystyrene standards. The optical and electrochemical properties of the polymers were examined by UV-vis absorption spectroscopy and cyclic voltammetry (CV). CV of the polymer films was performed on Pt plate in MeCN solution containing 0.10 M n-Bu_4NPF_6 with scan rate of 0.10 V/s.

2.3 EPR measurements

Room temperature (RT, T = 295 K) EPR measurements were done on both polycrystalline and thick film PTB7 samples using a EMX-220 X-band (ν = 9.4 – 9.8 GHz) spectrometer (Bruker Biospin, Rheinstetten, Germany) equipped with a Bruker ER 4102ST rectangular TE_{102} resonator and an Agilent 53150A frequency counter. Densities of paramagnetic centers N_s were determined by comparison of doubly integrated intensities of EPR lines from the samples under study with the intensity of the ERP signal of the purified 5 nm detonation nanodiamond powder with known density of S = 1/2 paramagnetic centers $N_s = 6.3 \times 10^{19}$ spin/g [20]. Bruker's WIN-EPR and SimFonia as well as Origin (OriginLab Corp., Northampton, USA) software were used for processing and simulation of EPR spectra.

Dark EPR spectra were measured on both initial polymer powders and films deposited on Si substrate. Prior to measurements all samples were kept under nitrogen atmosphere and in dark conditions. EPR spectra of PTB7 powders were recorded at the following instrumental conditions: non-saturating microwave power P_{MW} = 0.2 mW, 100 KHz magnetic field modulation amplitude A_{mod} = 0.03 mT, receiver gain = 2×10^5, number of coherent acquisitions n_{aqc} = 25). In Figure 1(a) densities of these spectra are normalized per 1 mg and, thus, reflect real spin densities in the samples under study. Due to both smaller effective weights of the polymer films as well as strong non-resonance absorption of microwave by the silicon substrate, the PTB7 film samples provide significantly less intensive EPR signals. For better accuracy of spin density estimation EPR spectra of films as well as the corresponding detonation nanodiamond reference sample, attached to the same substrate, were recorded in partially saturating (P_{MW} = 5 mW) and over-modulated (A_{mod} = 0.3 mT) conditions with receiver gain = 2×10^6 and n_{aqc} = 100.

2.4 OPV fabrication and characterisation

Inverted OPV devices were initially prepared in a clean room environment using indium tin oxide (ITO) coated glass substrates (R_s = 16 Ω/square, transparency=84% purchased from Xinyan Ltd.) that were first cleaned using deionised water, acetone and isopropanol in an ultrasonic cleaner, then treated in a UV-ozone reactor with oxygen plasma for 10 minutes. A zinc oxide (Zn) electron transporting layer was prepared from zinc acetate dehydrate (109 mg) dissolved in 2-methoxyethanol (1 ml) and ethanolamine (0.03 ml) solution, which was spin-coated at 2000 rpm on the ITO substrate. The samples were then annealed in the presence of atmospheric air at temperatures of 150 °C for the Zn acetate to calcinate into ZnO. Active layer BHJ blends using PTB7 (as a donor) and [6,6]-Phenyl-C_{71}-butyric acid methyl ester (C_{71}-PCBM) (as an acceptor) with weight ratios 1:1.5 were prepared and mixed with chlorobenzene solvent with a concentration of 30 mg/mL. Initial trials showed varying

blend ratio and concentration for different PTB7 polymers led to the same optimal blend. Therefore, all results were obtained with PTB7 polymers which were prepared with the same ratio and concentration. To improve the performance and to be consistent with other reports, the processing additive 1,8-diiodoctane (DIO) was dissolved into the blend at a concentration of 2.5% [14-17]. Prior to coating, the blend was allowed to dissolve for 1 hour on a hot plate at 45°C. Samples were transferred into a nitrogen atmosphere glovebox ([O_2], < 1ppm; [H_2O], <100ppm), where the active layers was applied by spin-casting from a 45°C solution. The active layer were annealed at 45°C for 15 minute before thermal evaporation of the cathode was performed through a shadow mask to define device area and consisted of 8 nm of MoO_3 and 100 nm of silver (Ag).

Devices were checked for initial performance prior to lifetime testing. The measurement system used to characterize the devices consisted of a Newport solar simulator with 100 $mWcm^{-2}$ AM1.5G output (calibrated using a silicon reference cell from RERA in the Netherlands. The open circuit Voltage (V_{oc}), short-circuit current density (J_{SC}), fill factor (FF) and PCE values are averaged from six cells (for each polymer). The devices were then placed under a halogen light source of 1 sun (calibrated by the silicon reference cell) for light soaking. Devices were kept at open circuit in between measurements and I-V measurements were made every 20 minutes, with more details of the procedure reported elsewhere [18]. This was conducted in accordance with ISOS-L-2 standards [18]. Devices were measured until the PCE reached 10% of its initial value.

3. Results

3.1 Material characterisation

PTB7 has been synthesized via Stille coupling reactions using two different palladium complex catalysts, $Pd_2(dba)_2$ or $Pd(PPh_3)_4$, giving **PTB7-1** and **PTB7-3**, respectively, as shown in Scheme 1. For a comparison, **PTB7-2** and **PTB7-4** were purchased from Lumtec Inc., Taiwan and Ossila Ltd., UK, respectively. The polymer notation is in ascending order of the molecular weight (**PTB7-1** and **PTB7-4** possess the lowest and the highest molecular weight, respectively). These values and the polymer polydispersity indexes (PDI) are summarized in Table 1 and Figure S1 in the supporting information.

The absorption spectra of the PTB7 samples dissolved in THF and in thin film form are presented in Figure S2 (see also Table 1). The variation in absorption is moderate and indicates that the optical differences between the polymers should not induce large variations in the device performance. The optical band gap (E_g) was estimated from the onset of the absorption spectra in thin film. **PTB7-3** shows the lowest λ_{max} and exhibits a broad absorption peak; therefore, it gives lower E_g of 1.57 eV than others (E_g = 1.66-1.67 eV). This is desirable from a photovoltaic point of view as it improves spectral match between the AM1.5G sunlight and the polymer absorption spectra. HOMO and LUMO levels were estimated from absorption and electrochemical measurements. For donor materials in OPV, deeper HOMO levels are preferred [19] and based on this assertion, **PTB7-4** is likely to be the best candidate, however, the data indicate that only a moderate difference in solar cell performance should be observed between **PTB7-1 – 4** samples.

3.2 EPR of powders and films

Figure 1(a) shows dark EPR spectra of PTB7 powders of various molecular weights recorded at the same instrumental conditions (see Methods). These spectra demonstrate the same polycrystalline pattern typical for S = 1/2 paramagnetic species in rhombically distorted surrounding having effective g-factors g_1 = 2.0064±0.0002, g_2 = 2.0048±0.0002 and g_3 = 2.00384±0.0002. At P_{MW} > 1 mW on both sides of the main signal several broad hyperfine lines split by ~0.4 mT are observed. Signals of similar shape have been recently reported for photothermally aged PTB7 films [11]. Simulation of this spectrum using tentative rhombically distorted radical structure with 6 I = 1/2 nuclei in surrounding, provides the following Spin-Hamiltonian parameters: g_1 = 2.0068, g_2 = 2.0038, g_3 = 2.0026, $a_1 = a_2 < 0.06$ mT and a_3 = 0.36 mT (see Figure S4). Electron spin-lattice and spin-spin relaxation times were estimated from the saturation curves and found to be (with ±30% estimation error) $T_{sl} = 1.4\times10^{-6}$ s and $T_{ss} = 1.4\times10^{-8}$ s, respectively. EPR spectra of film samples being recorded under alternative instrumental conditions (see Methods) provide the same EPR patterns as their initial powders (spectra not shown).

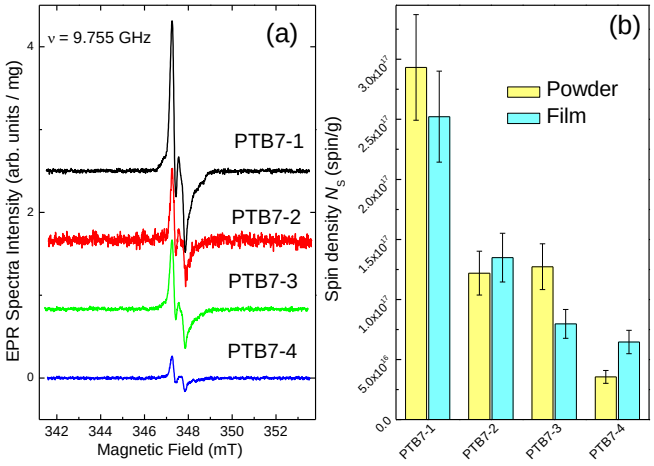

***Figure 1**. (a) X-band RT dark EPR spectra of PTB7 powders recorded at P_{MW} = 0.2 mW, A_{mod} = 0.03 mT, receiver gain = 2 × 10^5, n_{aqc} = 25 and ν = 9.755 GHz. Background signals are subtracted, vertical scale is normalized per unit mass, spectra are vertically shifted for better presentation, differences in signal-to-noise ratios are due to variations in the weight of powders under study; (b) spin densities N_S of paramagnetic defects in PTB7 powders (yellow bars) and films (magenta bars).*

Figure 1(b) and Table 2 summarize densities of paramagnetic defects (positive polarons) in the samples, N_s, and evidence that in both powders and films the N_s density correlates inversely with the molecular weight: as lower is M_n as higher is N_s. This means that PTB7 samples do not

incorporate spin-active units in their monomer structure and the observed radical defects present mostly on the polymer chain ends. Moreover, all results obtained on films correlated well with the OPV cell performance (see Table 2 and discussion below).

Table 2 *Summary of defect concentrations in various PTB7 samples performance of PTB7:C_{71}-PCBM OPV cells produced on their basis*

Polymer samples	M_n (M_w/M_n)	Defect spin density N_S (spin/g)[a]		V_{OC} (V)[b]	J_{SC}[c] (mA/cm^2)	Fill factor	PCE (%)	$t_{1/2}$[d] (hours)
		Powder	Film					
PTB7-1	41200 (2.55)	2.9×10^{17}	2.5×10^{17}	0.73±0.01	10.1±0.2	0.55±0.01	4.02±0.10	29.8
PTB7-2	83300 (2.83)	1.2×10^{17}	1.3×10^{17}	0.73±0.01	12.1±0.2	0.56±0.01	4.92±0.05	31.5
PTB7-3	108,900 (2.56)	1.3×10^{17}	8.0×10^{16}	0.71±0.01	13.9±1.0	0.62±0.03	6.04±0.3	56.5
PTB7-4	215700 (2.46)	3.6×10^{16}	6.5×10^{16}	0.70±0.01	15.7±0.5	0.61±0.02	6.71±0.29	98.8

[a] Errors in spin density determination do not exceed ± 15%, [b] Open circuit Voltage, [c] Short-circuit current density, [d] Half lifetime of the OPV under 1 sun irradiation.

3.3 OPV performance

Figure 2 shows the current density-voltage (*J-V*) characteristics of the BHJ OPV cells fabricated with **PTB7-1,-2, -3 and -4** and C_{71}-PCBM. Averaged principle parameters of these cells are summarized in Table 2. It appears that the highest molecular weight polymer (**PTB7-4**) leads to the highest PCE of 6.71% whilst the lowest molecular weight polymer (**PTB7-1**) leads to the poorest OPV performance (PCE = 4.02%). The medium molecular weight polymer, i.e. **PTB7-2** and **PTB7-3** showed medium PCE of 4.92% and 6.04%, respectively. The observed improvement in PCE with the M_n increase is caused mostly by differences in J_{sc}. Since the absorption spectra of the samples are relatively similar, we explain this by two reasons. First, relationships between M_n, N_S and J_{sc} indicate that samples with higher M_n contain fewer recombination centers in the polymer moiety of the photoactive layer and thus exhibit higher photocurrents.

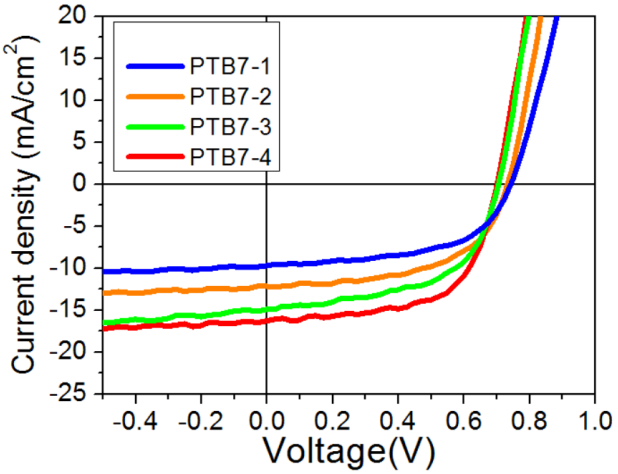

Figure 2*. J–V characteristics of OPV devices fabricated with polymers* ***PTB7 1 - 4*** *under AM1.5G illumination*

Second, this trend can also be equated to differences in the morphology of the photoactive layer. Lower M_n samples have smaller donor/acceptor interface area and thus provide poorer exciton dissociation efficiency. This statement is supported by AFM images of the photoactive layers (Fig. 3 a, c, e, g). The highest molecular weight polymer i.e. **PTB7-4** (blended with C_{71}-PCBM) yielded the smoothest surface with Root Mean Square (RMS) roughness = 2.0 nm (Fig. 3g) whilst the low molecular weight one i.e. **PTB7-1** showed the highest: 7.2 nm (Fig. 3a). The

PTB7-2 and **PTB7-3** polymer with moderate *M*n had an intermediate roughness of 5.9 nm and 4.9 nm, respectively. The discrete surface roughness is likely due to chain relaxation. Indeed, high molecular weight polymer, with high T_g, is difficult to move. Meanwhile, low molecular weight polymers, with lower T_g, are more mobile. Therefore they could relax from an as-spun ultra-smooth surface to a relatively rough surface during annealing and/or storage. Such relaxation could lead to undesirable phase separation [20] and the increased film roughness could cause the decrease in the J_{sc}.

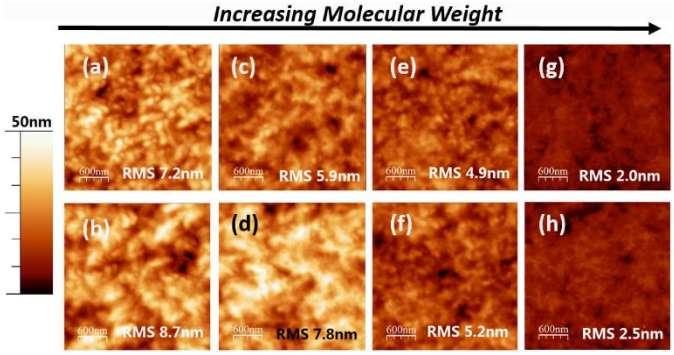

***Figure 3**. AFM images with indicated RMS values for PTB7: C_{71}-PCBM blends before (a, c, e, g) and after (b, d, f, h) light soaking. (a, b) **PTB7-1**: C_{71}-PCBM; (c, d) **PTB7-2**: C_{71}-PCBM; (e, f) **PTB7-3**: C_{71}-PCBM; (g, h) **PTB7-4**: C_{71}-PCBM.*

3.4 OPV performance

Lifetime stability tests for non-encapsulated devices were carried out under continuous illumination at 1 sun (Figure 4). Overall, the device fabricated with the high molecular weight polymer (i.e. **PTB7-4**, M_n= 216 k) possessed the highest stability, where the time to reach 50% of its initial value ($t_{1/2}$) was recorded at 96 hours. As the molecular weight of the polymer decreased, the stability of the devices appeared to reduce, as evidence by the fall in $t_{1/2}$ values. The decrease observed in PCE seems to be determined primarily by a drop in J_{sc} and supplemented by the decrease in FF.

Difference in morphological degradation in the active layer of the cells (Figure 3) may be among the reasons for the variation in *J*sc degradation rates. Considering the topography before and after light soaking, it is clear that the most significant changes were observed for the lower molecular weight polymers. The RMS rose from 7.2 nm to 8.98 nm for **PTB7-1** (Figures 3 a, b) and from 5.9 nm to 7.8 nm for **PTB7-2** (Figures 3 c, d). At the same time, the **PTB7-3** and **PTB7-4** showed moderate increases of less than 0.5 nm (Figures 3 e-h). As discussed above, a drastic change of the photoactive layer morphology could lead to undesirable donor-acceptor interfaces and could be a reason for the rapid drop in J_{sc} in **PTB7-1** and **PTB7-2** during light soaking.

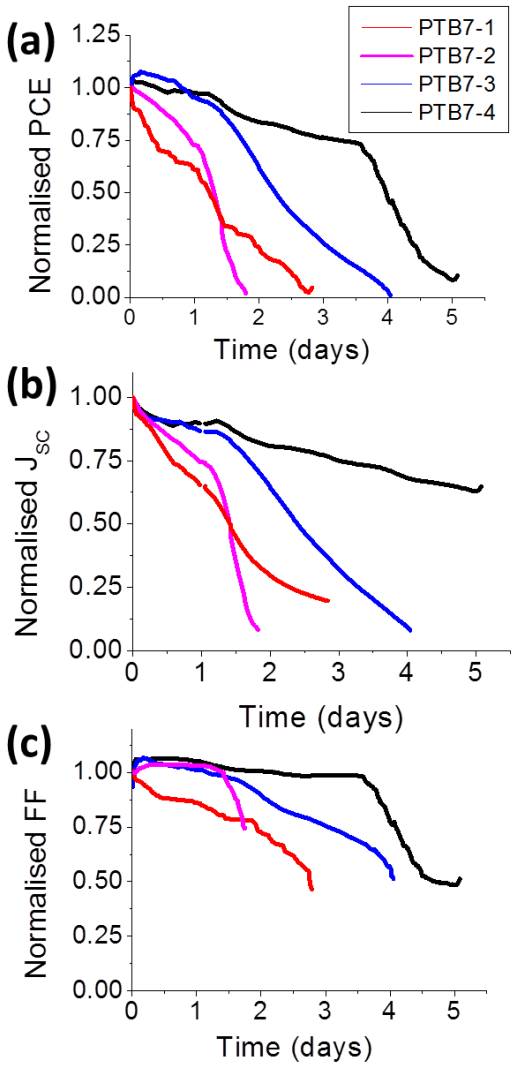

***Figure 4**: Device characteristics for non-encapsulated **PTB7 1-4**:C_{71}-PCBM inverted solar cells as a function of time under illumination of 1 sun. Each parameter was normalised to the initial value at the start of the aging process.*

On the other hand, the observed correlation between the cell PCE and lifetime suggests a general trend: the more efficient cells should be more stable. Indeed, photoinduced degradation of PV devices under operation is caused by sunlight. The more incident sunlight power converted to electrical power, the less remains for activation of degradation. During operation of polymer PVs, some fraction of the excitons generated under sunlight undergo non-radiative quenching leading to the photochemical degradation [11]. Efficient PV conversion due to the donor-acceptor charge transfer suppresses this process. Indeed, adding acceptor (PCBM) to the polymer blends was found to slow considerably the polymer photochemical degradation, presumably via sub nanosecond quenching of the reactive excited state by forming a lower energy charge transfer complex [21-23]. On the other hand, in small-molecule fullerene OPV cells, photochemical degradation of fullerenes was reported to occur by the same mechanism in both bi-layer and

BHJ devices [24]. However, the process in the BHJ is slower due to more rapid exciton quenching by charge-transfer.

At the present stage of research, it is probably too early to formulate this conclusion as a general rule. However, it should be taken into account for future development of various novel PV technologies (including OPV, and perovskite-based cells) and checked in further research.

Conclusions

In summary, we produced a number of PTB7 samples with various molecular weights (M_n ~ 40-220 k) and presented material characteristics and photovoltaic performance and lifetime of OPV devices fabricated with these samples. EPR spectroscopy revealed an inverse correlation between M_n and the densities of paramagnetic defects N_s in both powders and films of PTB7. This indicates that the observed radical defects present mostly on the polymer chain ends. Moreover, we demonstrated a gradual improvement in the PCE of PTB7:C_{71}-PCBM OPV cells with the increase of M_n of PTB7 due to increases in the cell short-circuit current, J_{sc}. We attributed this effect to the lower density of recombination centers and better photoactive layer morphology in the samples with higher M_n. Finally, the correlation between PCE and stability of the OPV cells was documented, showing improvement of the OPV lifetime by ~ 300% for high M_n samples.

Acknowledgements

JK and EK would like to acknowledge the support of support of the European Commission's StableNextSol COST Action MP1307. JK would like to thank Sêr Cymru national research network in Advanced Engineering and Materials.

References

1 You, J., Dou, L., Yoshimura, K., Kato, T., Ohya, K., Moriarty, T., ... & Yang, Y. (2013). A polymer tandem solar cell with 10.6% power conversion efficiency. *Nature communications*, *4*, 1446.

2 Bundgaard, E., Helgesen, M., Carlé, J. E., Krebs, F. C., & Jørgensen, M. (2013). Advanced functional polymers for increasing the stability of organic photovoltaics. *Macromolecular Chemistry and Physics*, *214*(14), 1546-1558.

3 Kaur, N., Singh, M., Pathak, D., Wagner, T., & Nunzi, J. M. (2014). Organic materials for photovoltaic applications: Review and mechanism. *Synthetic Metals*, *190*, 20-26.

4 Mazzio, K. A., & Luscombe, C. K. (2015). The future of organic photovoltaics. *Chemical Society Reviews*, *44*(1), 78-90.

5 Gevorgyan, S. A., Madsen, M. V., Roth, B., Corazza, M., Hösel, M., Søndergaard, R. R., …& Krebs, F. C. (2015). Lifetime of Organic Photovoltaics: Status and Predictions. *Advanced Energy Materials*.

6 Angmo, D., & Krebs, F. C. (2015). Over 2 Years of Outdoor Operational and Storage Stability of ITO-Free, Fully Roll-to-Roll Fabricated Polymer Solar Cell Modules. *Energy Technology*, *3*(7), 774-783.

7 He, Z., Zhong, C., Su, S., Xu, M., Wu, H., & Cao, Y. (2012). Enhanced power-conversion efficiency in polymer solar cells using an inverted device structure. *Nature Photonics*, *6*(9), 591-595

8 Liang, Y., Xu, Z., Xia, J., Tsai, S. T., Wu, Y., Li, G., ... & Yu, L. (2010). For the bright future—bulk heterojunction polymer solar cells with power conversion efficiency of 7.4%. *Advanced Materials*, *22*(20), E135-E138

9 Razzell-Hollis, J., Wade, J., Tsoi, W. C., Soon, Y., Durrant, J., & Kim, J. S. (2014). Photochemical stability of high efficiency PTB7: PC 70 BM solar cell blends. *Journal of Materials Chemistry A*, *2*(47), 20189-20195.

10 Balderrama, V. S., Sanchez, J. G., Estrada, M., Ferre-Borrull, J., Pallares, J., & Marsal, L. F. Relation of Polymer Degradation in Air With the Charge Carrier Concentration in PTB1, PTB7, and PCBM Layers Used in High-Efficiency Solar Cells.

11 Frolova L. A., Piven N. P., Susarova D. K., Akkuratov A. V., Babenko S. D., & Troshin P. A. (2015). EPR spectroscopy for monitoring the photochemical and thermal degradation of conjugated polymers used as electron donor materials in organic bulk heterojunction solar cells *Chem. Commun. 51*, 2242-2244

12 D.K. Susarova, N. P. Piven, A. V. Akkuratov, L. A. Frolova, M. S. Polinskaya, S.A. Ponomarenko, S. D. Babenkob and Pavel A. Troshin. 2015. EPR spectroscopy as a powerful tool for probing the quality of conjugated polymers designed for photovoltaic applications. *Chem. Commun. 51*, 2239-2241.

13 http://stablenextsol.eu/

14 Scharber, M. C., Muhlbacher, D., Koppe, M., Denk, P., Waldauf, C., Heeger, A. J., & Brabec, C. J. (2006). Design rules for donors in bulk-heterojunction solar cells-towards 10% energy-conversion efficiency. *Advanced Materials*, *18*(6), 789.

15 Lou, S. J., Szarko, J. M., Xu, T., Yu, L., Marks, T. J., & Chen, L. X. (2011). Effects of additives on the morphology of solution phase aggregates formed by active layer components of high-efficiency organic solar cells. *Journal of the American Chemical Society*, *133*(51), 20661-20663.

16 Jørgensen, M., Norrman, K., Gevorgyan, S.A., Tromholt, T., Andreasen, B., Krebs, F.C. (2012) Stability of Polymer Solar Cells, *Adv. Mater.,* 24, 580-612.

17 Brabec, C.J., Zerza, G., Cerullo, G., Silvestri, S.D., Luzzati, S., Hummelen, J.C., Sariciftci, S. (2001). Tracing photoinduced electron transfer process in conjugated polymer/fullerene bulk heterojunctions in real time. *Chem. Phys. Lett.,* 340, 232-236.

18 Manceau, M., Chambon, S., Rivaton, A., Gardette, J.-L., Guillerez, S., Lemaıtre, N.E. (2010) Effects of long-term UV–visible light irradiation in the absence of oxygen on P3HT and P3HT:PCBM blend. *Sol. Ener. Mater. Sol. Cells*, 94, 1572–1577.

19 Burlingame, Q., Tong, X., Hankett, J., Slootsky, M., Chen, Z., Forrest, S.R. (2015). Photochemical origins of burn-in degradation in small molecular weight organic photovoltaic cells. *Energy Environ. Sci*., 8, 1005-1010.

20 Osipov V. Yu., Shames A. I., Enoki T., Takai K., Baidakova M. V., & Vul' A. Ya. (2007). Paramagnetic defects and exchange coupled spins in pristine ultrananocrystalline diamonds. *Diamond Relat. Mater. 16*, 2035 - 2038

21 Liu, F., Zhao, W., Tumbleston, J. R., Wang, C., Gu, Y., Wang, D., ... & Russell, T. P. (2014). Understanding the morphology of ptb7: pcbm blends in organic photovoltaics. *Advanced Energy Materials*, *4*(5).

22 Lou, S. J., Szarko, J. M., Xu, T., Yu, L., Marks, T. J., & Chen, L. X. (2011). Effects of additives on the morphology of solution phase aggregates formed by active layer components of high-efficiency organic solar cells. *Journal of the American Chemical Society*, *133*(51), 20661-20663.

23 Waters, H., Bristow, N., Moudam, O., Chang, S. W., Su, C. J., Wu, W. R., ... & Kettle, J. (2014). Effect of processing additive 1, 8-octanedithiol on the lifetime of PCPDTBT based Organic Photovoltaics. *Organic Electronics*, *15*(10), 2433-2438.

24 Kettle, J., Waters, H., Ding, Z., Horie, M., & Smith, G. C. (2015). Chemical changes in PCPDTBT: PCBM solar cells using XPS and TOF-SIMS and use of inverted device structure for improving lifetime performance. *Solar Energy Materials and Solar Cells*, *141*, 139-147.
25 Reese, M. O., Gevorgyan, S. A., Jørgensen, M., Bundgaard, E., Kurtz, S. R., Ginley, D. S., ... & Krebs, F. C. (2011). Consensus stability testing protocols for organic photovoltaic materials and devices. *Solar Energy Materials and Solar Cells*, *95*(5), 1253-1267